ResearchGate

See discussions, stats, and author profiles for this publication at: https://www.researchgate.net/publication/40818728

Cooperative Strengthening of an Intramolecular O—H···O Hydrogen Bond by a Weak C—H···O Counterpart: Matrix-Isolation Infrared Spectroscopy and Quantum Chemical Studies on 3-Methyl-...

ARTICLE *in* THE JOURNAL OF PHYSICAL CHEMISTRY A · FEBRUARY 2010

Impact Factor: 2.69 · DOI: 10.1021/jp907881b · Source: PubMed

CITATIONS
18

READS
20

4 AUTHORS:

Amit Kumar Samanta
University of Southern California
22 PUBLICATIONS **163** CITATIONS
SEE PROFILE

Prasenjit Pandey
Indian Association for the Cultivation of Sci...
19 PUBLICATIONS **109** CITATIONS
SEE PROFILE

Biman Bandyopadhyay
Malaviya National Institute of Technology ...
16 PUBLICATIONS **91** CITATIONS
SEE PROFILE

Tapas Chakraborty
Indian Association for the Cultivation of Sci...
107 PUBLICATIONS **853** CITATIONS
SEE PROFILE

Available from: Biman Bandyopadhyay
Retrieved on: 26 January 2016

Cooperative Strengthening of an Intramolecular O—H···O Hydrogen Bond by a Weak C—H···O Counterpart: Matrix-Isolation Infrared Spectroscopy and Quantum Chemical Studies on 3-Methyl-1,2-cyclohexanedione

Amit K. Samanta, Prasenjit Pandey, Biman Bandyopadhyay, and Tapas Chakraborty*

Department of Physical Chemistry, Indian Association for the Cultivation of Science, Jadavpur, Kolkata 700032, India

Received: January 13, 2009; Revised Manuscript Received: November 21, 2009

Matrix-isolation infrared spectra of 1,2-cyclohexanedione (CD) and 3-methyl-1,2-cyclohexanedione (3-MeCD) were measured in a nitrogen matrix at 8 K. The spectral features reveal that, in the matrix environment, both molecules exist exclusively in the monohydroxy tautomeric form, which is stabilized by an intramolecular O—H···O═C hydrogen bond (HB). The ν_{O-H} band of the enol tautomer of 3-MeCD appears at a relatively lower frequency and displays a somewhat broader bandwidth compared to that of CD, and these spectral differences between the two molecules are interpreted as being due to the formation of an interconnected C—H···O HB, where the enolic oxygen is the HB acceptor and one of the C—H covalent bonds of the methyl group is the HB donor. Electronic structure calculations at the B3LYP/6-311++G**, MP2/6-311++G**, and MP2/cc-pVTZ levels predict that this tautomer (enol-2) is ∼3.5 kcal/mol more stable than a second enolic form (enol-1) where such interconnected H-bonding is absent. Theoretical analysis with a series of molecules having similar functional groups reveals that part of the excess stability (∼1 kcal/mol) of enol-2 originates from a cooperative interaction between the interconnected C—H···O and O—H···O HBs. In the IR spectrum, a weak band at 3007 cm^{-1} is assigned to ν_{C-H} of the methyl C—H bond involved in the H-bonded network. The spectra predicted by both harmonic and anharmonic calculations reveal that this transition is largely blue-shifted compared to the fundamentals of the other two methyl C—H stretching frequencies that are not involved in H-bonding. The conclusions are corroborated further by natural bond orbital (NBO) analysis.

1. Introduction

Cooperativity is an important attribute of interconnected hydrogen bonds (HBs).[1−4] The effect refers to enhanced stability of a system containing two or more interconnected HBs, where the total HB energy is larger than the sum of the energies of same number of equivalent but isolated HBs. The excess stabilization in the first case originates as a result of mutual polarization of the covalent bonds involved in H-bonding, and classic examples include small cyclic clusters of water, where both the stability and the O—H stretching frequencies depend on cluster size, $(H_2O)_n$.[5,6] In recent years, attention has been focused on investigating the existence of such effects in systems where C—H groups are HB donors.[7−10] On the basis of crystallographic analyses and electronic structure calculations, cooperative stabilization has been inferred in crystals of several molecules.[11−13] However, direct spectroscopic evidence for cooperativity, in terms of spectral shifts of stretching fundamentals of the covalent HB donor groups, is rather scarce. Recently, Wallen et al. investigated the role of C—H···O hydrogen bonds in the CO_2-philic stabilization in complexes between CO_2 and acetaldehyde by use of Raman spectroscopy.[14] The effect was also investigated by quantum chemistry methods for complexes of CO_2 with formaldehyde, methyl acetate, acetic acid, and so on.[10] The cooperative effects of the C—H···O interaction on adjacent O—H···O HBs were investigated theoretically for the homodimers of acetic acid and acrylic acid and the mixed dimer between acetic acid and acetamide.[15] However, to our knowledge, direct spectroscopic evidence of cooperative stabilization in such systems has not been reported to date.

In the present article, we report the infrared spectroscopic signatures of cooperative interactions between a classical O—H···O HB and a weak C—H···O HB in the enol tautomer of a diketo compound. Infrared spectroscopy has been extensively used to study the keto/enol tautomers of a large variety of molecules.[16−20] In the present study, the system selected to demonstrate the effect is the monohydroxy tautomer of 3-methyl-1,2-cyclohexanedione (3-MeCD), a natural product found in coffee beans,[21] where these two bonds are interconnected with each other, and the spectral features are compared with those of its parent molecule 1,2-cyclohexanedione (CD), where the C—H···O bond is absent. For the latter molecule, electron energy loss spectroscopy,[22] ion cyclotron resonance mass spectrometry,[23] and electron diffraction measurements in the vapor phase[24] have revealed that, in the gas phase, the molecule exists primarily in an enol tautomeric form with an intramolecular O—H···O HB. In 3-MeCD, evidence is provided for an additional C—H···O hydrogen bond between a methyl C—H (donor) and the oxygen atom (acceptor) of the keto/enol group. A nearly isomeric molecule, 4-methylcyclohex-4-ene-1,2-dione (4-MeCED), in which such intramolecular C—H···O H-bonding is not possible, is used as a reference system. Electronic structure calculations at different levels of theory were performed to aid in the interpretation of the measured spectra.

* Corresponding Author.

10.1021/jp907881b © 2010 American Chemical Society
Published on Web 12/31/2009

2. Materials and Methods

2.1. Experimental Section. CD and 3-MeCD were obtained from Aldrich and purified further by vacuum distillation. The FTIR spectra were recorded using a Bruker IFS66S Fourier transform infrared spectrometer equipped with a deuterated triglycine sulfate (DTGS) detector and a KBr beam splitter. The instrument resolution of the spectrometer used for the measurements presented here was 1 cm^{-1}. The spectrometer compartment was constantly purged with dry N_2 to remove water vapor and CO_2. For matrix-isolation studies, a gas mixture consisting of the sample vapor and ultrahigh-purity nitrogen (N_2) was condensed onto a thin KBr window cooled at ~8 K by a closed-cycle helium refrigerator (Advanced Research Systems, Inc., model DE202). The spectra were recorded using several gas mixtures containing different partial pressures of the sample vapor in nitrogen. Care was taken to avoid association of the sample molecules in the matrix.

2.2. Theoretical Calculations. Optimization of the geometries of all of the tautomers of CD and 3-MeCD was performed by the B3LYP, B3PW91, and MP2 theoretical methods using 6-311++G** basis set. The correlation-consistent cc-pVTZ-type basis set was also used to perform MP2 calculations. The vibrational frequencies of all possible tautomer of the two molecules were calculated by the above-mentioned theoretical methods in harmonic approximation. Two different scale factors were used to correlate the measured frequencies with the predicted ones. For the frequencies predicted by the MP2 method, the suitable scale factor for the ν_{O-H} and ν_{C-H} regions was found to be 0.943, and for the fingerprint region, the scale factor was 0.976. For frequencies predicted by the B3LYP/6-311++G** method, the required scale factors for the two regions were found to be 0.958 and 0.977, respectively. We also performed anharmonic frequency calculations for the hydrogen-bonded enol tautomer of 3-MeCD by the B3LYP/6-311++G** and B3PW91/6-311++G** methods. Natural bond orbital (NBO) analysis was performed to calculate the natural charges at the donor−acceptor sites, hybridization characteristics of various bonding orbitals, and hyperconjugation interaction energies corresponding to different hydrogen-bonding sites. All calculations presented here were carried out using the Gaussian 03 program package.[25]

3. Results and Discussion

3.1. Structure and Stability of the Tautomers of 3-MeCD. The optimized structures of the three possible tautomers of 3-MeCD are shown in Figure 1, and the relative energies of these species are presented in Table 1. A doubly hydrogen-bonded enol tautomer A3, where the enolic group acts simultaneously as the donor for the classical intramolecular O—H···O HB and the acceptor for a weak intramolecular C—H···O HB involving the methyl group, is predicted to be the most stable, and it is favored over the diketo species (A1) by 7.8 kcal/mol. Some relevant geometric parameters of A3, along with those of the monohydroxy tautomer of CD (B2), are listed in Table 2. Furthermore, we show below that the ν_{C-H} transition corresponding to the methyl C—H bond involved in the C—H···O H-bonding experiences a kind of blue shifting compared to the other two C—H bonds of the methyl group, which are oriented out of the molecular plane. A second monohydroxy tautomer of 3-MeCD (A2), where the enolic group is only a HB donor to the carbonyl oxygen (A2), is predicted to be less stable by 3.6 kcal/mol.

Among the different tautomers of CD and 3-MeCD shown in Figure 1, the shortest O—H···O HB was predicted for the A3 tautomer of 3-MeCD (2.043 Å). The HB length of the A2 tautomer is 2.056 Å, and it is still longer in the case of B2 tautomer of the parent molecule CD (2.07 Å). These geometrical parameters imply that the methyl group in the vicinity of the enolic OH group of A3 bolsters the O—H···O HB. Furthermore, the distance between H^a and the enolic oxygen (O^8) atom was optimized as short as 2.45 Å, which is clearly within the favorable range of formation of a C—H···O HB involving the C—H bond of the methyl group directed toward the enolic OH. On the other hand, this distance between the two said atoms in the case of the A2 tautomer is much larger (2.62 Å). Another noteworthy point is that the three C—H bond lengths of the methyl group of the A3 tautomer are not same. The C^{10}—H^a bond is much shorter (1.088 Å) than the two out-of-plane C—H bonds (1.096 Å). In the case of the A2 tautomer, the methyl C—H adjacent to the keto oxygen is also somewhat shorter (1.090 Å) than the other two C—H bonds (1.093 Å).

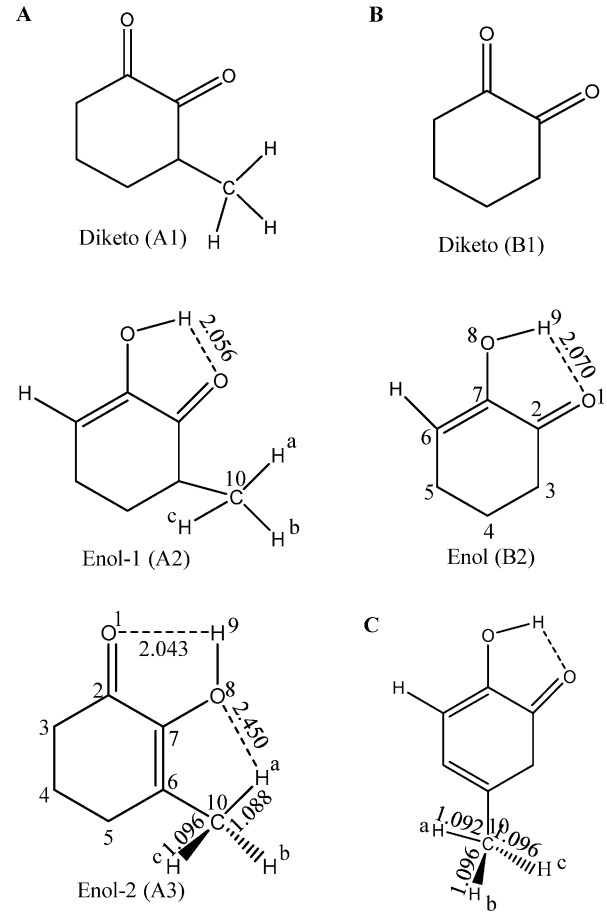

Figure 1. Optimized structures of the (A) three tautomers of 3-MeCD, (B) two tautomers of CD, (C) monohydroxy tautomer of 4-MeCED obtained by the B3LYP/6-311++G** method.

TABLE 1: Relative Energies (kcal/mol) of the Diketo and Monoenol Tautomers of CD and 3-MeCD Predicted by Calculations at the B3LYP/6-311++G and MP2/cc-pVTZ Levels of Theory**

		relative energy (kcal/mol)	
molecule	tautomeric species	B3LYP	MP2
3-MeCD	diketo (A1)	0	0
	enol-1 (A2)	−4.18	−4.07
	enol-2 (A3)	−7.79	−6.88
CD	diketo (B1)	0	0
	enol (B2)	−4.59	−4.55

TABLE 2: Some Important Geometrical Parameters of the Monoenol Tautomer of CD and 3-MeCD Calculated by the B3LYP/6-311++G Level**

		3-MeCD	
bond length (Å)	CD	A2	A3
O_1—C_2	1.222	1.223	1.225
C_2—C_7	1.483	1.484	1.476
C_7—O_8	1.356	1.356	1.362
O_8—H_9	0.972	0.973	0.973
C_6—C_7	1.344	1.343	1.350
C_{10}—H_a	–	1.090	1.088
C_{10}—H_b	–	1.093	1.096
C_{10}—H_c	–	1.093	1.096
O_1—H_9	2.070	2.056	2.043
O_8—H_a	–	–	2.454
O_1—H_a	–	2.620	–

3.2. Matrix-Isolated FTIR Spectra. The FTIR spectra of CD and 3-MeCD, recorded in a solid N_2 matrixes at 8 K, are shown in parts a and c, respectively, of Figure 2. The theoretical infrared spectra of the H-bonded enol tautomers of the two molecules (A3 and B2), calculated by the B3LYP/6-311++G** method, are presented in parts of b and d of the same figure to aid in assigning the vibrational bands in the two measured spectra. The calculated spectra are presented by scaling the predicted vibrational frequencies by a factor of 0.977 for the range of 400−2800 cm^{-1} and by 0.958 for 2800−4000 cm^{-1} range. The most intense bands displayed (Figure 2a,c) near 3460 cm^{-1} are assigned to O—H stretching fundamentals (ν_{O-H}) of the enol tautomers of the two diketones, and obvious red shifting of these bands compared to typical ν_{O-H} frequencies of the free OH group indicates that the enol group is intramolecularly hydrogen-bonded to the adjacent carbonyl (C═O) functional group in both systems. The harmonic frequencies (scaled) of this vibration of 3-MeCD predicted by the B3LYP/6-311++G** and MP2/6-311++G** methods are 3507 and 3510 cm^{-1}, respectively. The discrepancy of nearly 50 cm^{-1} between the measured and predicted frequencies is due to the significant anharmonic character of the intramolecularly H-bonded O—H stretching mode. A more accurate prediction for this mode

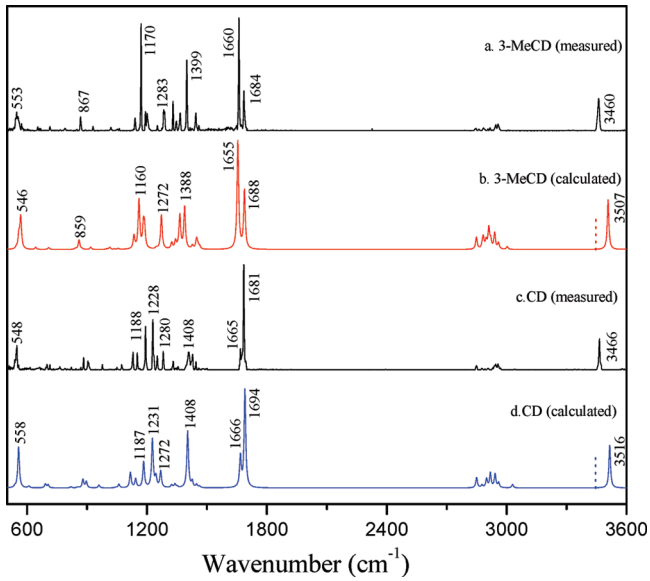

Figure 2. Infrared spectra of CD and 3-MeCD measured in N_2 matrixes and simulated by the B3LYP/6-311++G** method. The vertical dotted lines on the simulated spectra indicate ν_{O-H} frequencies predicted by anharmonic calculations at the same level.

frequency was obtained from anharmonic calculation; for example, the predicted frequency in the case of 3-MeCD for such a calculation at the B3LYP/6-311++G** level is 3443 cm^{-1}. A comparison between the harmonic and anharmonic frequencies for other IR-active vibrational modes is presented in Table 3.

In the spectral region of the carbonyl stretching fundamental ($\nu_{C=O}$), two closely spaced bands (doublet) are observed in each spectrum, and the same feature is also predicted by both harmonic and anharmonic calculations. Atom displacement vectors indicate that these two modes correspond to the in-phase and out-of-phase combinations of C═O and C═C stretching vibrations, which are mixed with the enolic O—H bending. In the case of 3-MeCD, the doublet components appear at 1660 and 1684 cm^{-1} with an intensity ratio of 3:1 (Figure 2a). However, in the IR spectrum of CD (Figure 2c), the relative intensity of the doublet components is reversed; that is, the higher-frequency component is nearly 4 times more intense than the lower-frequency component. The assignment of the fingerprint region of the spectrum of 3-MeCD is shown in Table 3.

Figure 3 shows the ν_{C-H} and ν_{O-H} regions of the two measured spectra in an expanded scale. The ν_{O-H} band of 3-MeCD appears distinctly broader and red-shifted (6 cm^{-1}) compared to that of CD. These features are indicatious of relatively stronger intramolecular O—H···O H-bonding in the former case. Consistent with these observations, our calculation at the MP2/6-311++G** level predicts that the O—H···O HB length of 3-MeCD is 0.03 Å shorter and ν_{O-H} is 9 cm^{-1} smaller compared to the corresponding values of CD. Calculation at the B3LYP/6-311++G** level also predicts similar differences (Table 2). Thus, the O—H···O HB of 3-MeCD is obviously strengthened by the presence of the adjacent methyl group.

In the spectral region of the ν_{C-H} transition, although the overall appearance of the two spectra is similar, the signatures of specific structural features of the two molecules are vividly displayed in the respective spectra. Thus, the three bands labeled h, a, and s in the measured spectrum of 3-MeCD, which are absent in the lower most panel (CD), are assigned to the three C—H stretching fundamentals of the methyl group. The band labeled e (3039 cm^{-1}) in the spectrum of CD is assigned to the ethylenic C—H stretching fundamental of the enol tautomer. In the former spectrum, the band labeled h (3007 cm^{-1}) is assigned to the ν_{C-H} transition of the methyl C^{10}—H^a bond, where H^a is H-bonded to the enolic oxygen atom (O^8). The other two bands denoted by s (2884 cm^{-1}) and a (2917 cm^{-1}) correspond to the symmetric and antisymmetric stretching fundamentals, respectively, of the two free C—H bonds (C^{10}—H^b and C^{10}—H^c) of the methyl group. The justification of these assignments is based primarily on correspondences observed between the measured and calculated frequencies. The frequencies predicted for the three said ν_{C-H} bands of the methyl group by anharmonic calculations at the B3PW91/6-311++G** level are presented in panel A and exhibit an excellent agreement with the measured band positions. In panels B and C, we present the bands calculated for the same three transitions by harmonic calculations at the B3PW91/6-311++G** (scale factor-0.954) and MP2/6-311++G** levels, and these also show good agreement with the measured band frequencies. Below, we rationalize first the origin of the differences for ν_{C-H} transitions of the in-plane and out-of-plane C—H bonds of the methyl group.

In the absence of any perturbation, the two antisymmetric C—H stretching vibrations of the methyl group in a symmetric molecular environment, such as that of CH_3Cl, are degenerate.[26] However, this degeneracy in the case of the A3 tautomer is

TABLE 3: Assignments of the Vibrational Bands in the Matrix-Isolation FTIR Spectrum of 3-MeCD

	calculated frequencies (cm^{-1})			
experimental frequency (cm^{-1})	B3LYP/6-311++G** (scaling 0.958/0.977)	MP2/6-311++G** (scaling 0.943/0.976)	anharmonic calculation B3LYP/6-311++G**	assignment
3460	3507	3510	3443	ν_{O-H}
3007	3002	3001	2990	ν_{C-H}(methyl)
2957	2958	2966	2948	ν_{C^3-H}
2946	2939	2951	2923	ν_{C^4-H}
2917	2920	2944	2899	ν^{asym}_{C-H}(methyl)
2906	2910	2895	2901	$\nu_{C^{4/5}-H}$
2884	2883	2881	2899	ν^{sym}_{C-H}(methyl)
2847	2848	2855	2840	ν_{C^5-H}
1684	1688	1681	1687	$(\nu_{C=O} + \nu_{C=C})_{OOP} + \delta_{O-H}$
1660	1655	1661	1653	$(\nu_{C=O} + \nu_{C=C})_{IP} + \delta_{O-H}$
1459	1455	1463	1458	δ_{C-H}(methyl)
1444	1435	1456	1445	δ_{C-H}(methyl)
1425	1428	1436	1438	δ_{C^3-H}(scissoring)
1399	1388	1408	1381	$\delta^{IP}_{O-H} + \delta_{C-H}$(methyl)
1366	1364	1373	1361	$\delta^{IP}_{O-H} + \delta_{C-H}$(methyl)
1347	1342	1353	1338	$\delta_{C-H} + \delta^{IP}_{O-H}$
1330	1324	1335	1322	δ_{C^5-H}(wagging) + δ^{IP}_{O-H}
1283	1272	1285	1277	δ_{C^3-H}(wagging)
1252	1247	1254	1245	$\delta_{O-H} + \nu_{C^2-C^7} + \delta_{C^3-H}$(wagging)
1192	1188	1192	1186	$\delta_{C^{3/5}-H}$(twist)
1170	1160	1176	1160	$\nu_{C-O} + \nu_{C-C}$
1140	1135	1138	1137	$\nu_{C-C} + \nu_{C-O}$
1061	1056	1059	1058	$\delta_{C^{3/5}-H}$(rocking)
1020	1013	1025	1014	δ_{C-H}(rocking)
930	918	927	924	$\delta_{O-H} + \nu_{C^3-C^4}$
867	859	867	865	$\nu_{C^2-C^7}$
850	841	844	851	$\delta_{C^{3/4/5}-H}$(rocking)
713	708	700	718	δ_{C-C}(ring)
652	643	648	646	δ_{C-C}(breathing)
571	568	561	570	δ^{op}_{O-H}
553	546	540	553	$\delta^{op}_{O-H} + \nu_{C-C}$(breathing)

lifted for two primary reasons: first, because of the intramolecular C—H···O H-bonding between the methyl H[a] and enolic oxygen (O[8]), and second, as a result of electronic conjugation of the two out-of-plane C[10]—H[b] and C[10]—H[c] bonds with the adjacent ethylenic π-bond network.[27] The latter factor is likely to induce elongation of the two out-of-plane methyl C—H bonds, and consequently, the corresponding ν_{C-H} frequencies are reduced. To assess the effect of the latter factor alone, that is, the effect of hyperconjugation when the H-bonding effect is absent, we performed geometry optimization and infrared spectrum calculation of the monohydroxy tautomer of 4-MeCED (Figure 1C), where the intramolecular C—H···O H-bonding is absent, but the π-conjugation remains unbroken. In the optimized geometry, the C[10]—H[b] and C[10]—H[c] bond lengths (1.096 Å) are predicted to be the same as in species A3, but the corresponding C[10]—H[a] bond length (1.092 Å) is relatively greater. The three methyl ν_{C-H} bands of the calculated IR spectrum of this molecule are shown in panel D of Figure 3. The frequencies for the symmetric and antisymmetric ν_{C-H} transitions are predicted to be nearly the same as those of A3 species, but the frequency of the h band is ~28 cm^{-1} smaller. The reduced frequency of the h band is consistent with the relatively greater bond length (1.092 Å) predicted for the C[10]—H[a] bond of 4-MeCED compared to that of 3-MeCD. Thus, the comparison indicates that the higher frequency of the h band of the latter species is the manifestation of C—H···O H-bonding, wherein ν_{C-H} blue shifting with concomitant C—H bond-length shortening is a common phenomenon.[28−38]

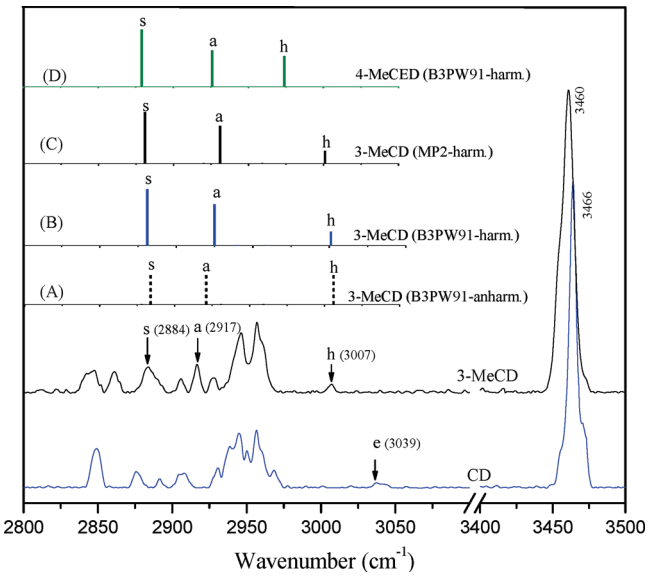

Figure 3. FTIR spectra in the C—H and O—H stretching fundamental region (2800−3500 cm^{-1}) of 3-MeCD (black) and CD (blue) isolated in N_2 matrixes at 8 K. The bands denoted by inverted arrows (s, a, and h) correspond to the three ν_{C-H} transitions of the methyl group of 3-MeCD. The corresponding transitions in the calculated IR spectra of 3-MeCD and 4-MeCED are shown in stick format.

In one modern view, the factors that contribute primarily to ν_{C-H} spectral shifts in a C—H···O H-bonded complex are the (i) long-range electrostatic interaction between the weakly polar C—H bond and the electron-rich O atom[1,2,39−41] and (ii) hyperconjugative charge transfer from the filled nonbonded orbitals of O (n_O) to the antibonding orbital of C—H (σ^*_{C-H}).[41−43] The latter interaction causes elongation of the C—H bond by increasing the population of its antibonding orbital and, thus,

induces red shifting of the C—H stretching fundamental. The interaction depends sensitively on the overlap of the two orbitals and, hence, the relative orientation of the donor−acceptor groups and their spatial separation. For the A3 tautomer of the present systems, the NBO analyses at the B3LYP/6-311++G** and MP2/6-311++G** levels predict that the hyperconjugation interaction energies between the $n(O^8)$ and $\sigma^*(C^{10}—H^a)$ orbitals are 0.14 and 0.11 kcal/mol, respectively. These values are rather small compared to that of a typical dimeric C—H···O HB complex reported in recent years.[41] Because the interaction energy depends on the effective overlap between the donor−acceptor orbitals, the restricted approach of the two intramolecular groups in the present system is responsible for the weak orbital overlap.

The electrostatic interaction between the donor−acceptor groups at the HB site causes repolarization of the C—H bond, giving rise to an increased partial positive charge ($\delta+$) on the H atom. In effect, according to Bent's rule, the carbon-centric orbital of the covalent bond might experience rehybridization resulting in increased s character in the hybrid orbital, which could be responsible for shortening of the C—H bond. Such a repolarization/rehybridization effect, which results in blue shifting of the C—H stretching frequency, is manifested predominantly when the hyperconjugation energy is rather smaller, as for the case of the A3 tautomer. A scrutiny of the natural charges on the H atoms of the methyl group and hybridization of the carbon-centric orbitals of the three methyl C—H bonds, as obtained from NBO analysis (see Supporting Information for details), reveals that the natural charge on the H^a atom (+0.23) is larger than that on the H^b and H^c atoms (+0.21). Likewise, the s character of the carbon hybrid orbital of the $C^{10}—H^a$ bond ($sp^{3.07}$) is larger than that of the other two ($C^{10}—H^b$ and $C^{10}—H^c$) bonds ($sp^{3.37}$). To verify that C—H···O H-bonding contributes to these differences, we also performed NBO analysis on 4-MeCED. The results show that the hybridization of the two out-of-plane C—H bond orbitals of this molecule are almost the same as that of the A3 tautomer (Supporting Information), but the hybridization of the in-plane C—H bond is significantly different, having relatively smaller s character. Furthermore, the NBO analysis on the A2 tautomer shows that the s character of the carbon hybrid orbital of the C—H bond directed toward the carbonyl oxygen is smaller ($sp^{3.15}$) than that of the $C^{10}—H^a$ bond of the A3 tautomer. These data indicate that the C—H···O H-bonding effect in the A2 tautomer is weaker than that in A3.

Cooperative Interaction between C—H···O and O—H···O Hydrogen Bonds. It was pointed out in the previous section that the ν_{O-H} band corresponding to the A3 tautomer of 3-MeCD appears broader and more red-shifted than that of CD, and we interpret these spectral features as the manifestations of a correlation between the interconnected C—H···O and O—H···O hydrogen bonds. In this section, we assemble the theoretical evidence in favor of this interpretation. The broadening of the ν_{O-H} band could arise as a result of fast vibrational dynamics of the molecule at the first excited stretching vibrational quantum level,[44] which, in 3-MeCD, is certainly influenced by the interconnected C—H···O HB, as this feature is absent in the spectrum of CD. The rotor effect of the methyl group, which arises because of the low methyl tortional barrier and the highly anharmonic nature of the tortional potential, could further accelerate the energy redistribution process, and that can also contribute spectral broadening.[45]

The relative energies of the three tautomers of 3-MeCD, presented in Table 1, indicate that the A3 tautomer is favored over the other enolic species A2 by ∼3.5 kcal/mol. We justify below providing with theoretical data that part (∼1 kcal/mol) of the excess stability of A3 originates from a cooperative interaction between the two interconnected HBs. First, it has been noticed that, if the methyl group is made to rotate by 60° from the most stable position, the energy of the system is increased by about 1 kcal/mol. An obvious reason for this change is the loss of CH···O hydrogen bonding and also ineffective hyperconjugation of the two out-of-plane methyl C—H bonds with the adjacent ethylenic group at 60° orientation. Scrutiny of the geometrical parameters reveals that, at the new position of the methyl group, the $O^8—H^9···O^1$ HB length is increased to 2.6 from 2.4 Å and there is also a small change in polarization of the enolic O—H bond, which is reflected in reduction of natural charges on the H (from +0.49 to +0.48) and O (from −0.69 to −0.68) atoms. Furthermore, NBO analysis shows that, among the three monoenol tautomers (A2, A3, and B2), A3 has the largest hyperconjugation energy and this energy is correlated with the orientation of the methyl group. As the methyl group is internally rotated, the hyperconjugation energy decreases and passes through a minimum at around 50° (Supporting Information). These effects indicate clearly the existence of a correlation between the two HBs.

To estimate the contribution of the cooperative stabilization for the two interconnected HBs in A3, we provide here a supporting theoretical analysis. The relative energies of the keto/enol tautomers of a series of molecules (Figure 4) were calculated, and from these data, one can infer that the contribution of the cooperative effect in A3 cannot be less than 1 kcal/mol. The required calculations were performed at the MP2/cc-pVTZ and B3LYP/6-311++G** levels.

(i) In the case of acetaldehyde (I), the calculations at the two said levels predict that the keto tautomer is more stable than the enol (I_{enol}) by ∼12 kcal/mol. However, this energy difference between the two tautomers is reduced to ∼10 kcal/mol in the case of propanaldehyde. In the latter case, the carbonyl and terminal methyl groups are separated by a methylene spacer, and in the enol tautomeric form, the methyl group can interact with the adjacent ethylenic group through a hyperconjugation mechanism; this effect is likely to be responsible for the extra stability of the enol form of propanaldehyde (II_{enol}). Here, the contribution of the hyperconjugation energy could be ∼2 kcal/mol. A scrutiny of the geometric parameters of II_{enol} reveals that the three C—H bond lengths of the methyl group are not same. The bond directed toward the enolic oxygen is coplanar with the vinyl group and somewhat shorter than the other two out-of-plane C—H bonds, whereas the latter two have the same bond length.

(ii) In the case of cyclohexanone (III), the keto tautomer is predicted to be favored over the enol (III_{enol}) by ∼8.0 kcal/mol. Interestingly, when a methyl group is incorporated at the 2 position of the ring (species IV), the keto/enol energy difference is reduced to ∼6.0 kcal/mol; that is, IV_{enol} is more stable than III_{enol} by ∼2 kcal/mol, similarly to the case of the enolic pair of acetaldehyde and propanaldehyde. Furthermore, here, the orientation of the three C—H bonds of the methyl group with respect to the ethylenic plane is the same as in II_{enol}. The C—H bond directed toward the enolic oxygen is shorter than the other two methyl C—H bonds. The same factor (i.e., methyl hyperconjugation) could again be the primary factor for the preferential stability IV_{enol} over III_{enol}. On the other hand, in the case of 3-methyl cyclohexanone (V), where the methyl group cannot be involved into hyperconjugation interaction because of its position in the ring, the keto/enol energy difference is increased again to ∼8 kcal/mol. Therefore, on the basis of this

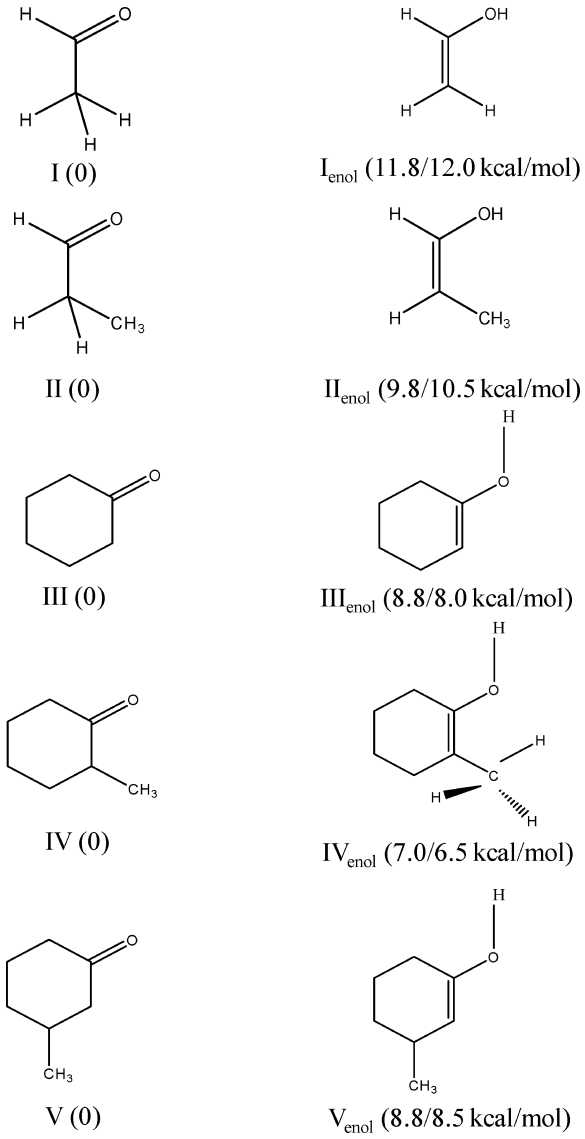

Figure 4. Keto/enol tautomers of five model carbonyl compounds used to estimate the methyl hyperconjugation energy. The data in parentheses in the right-hand column are the energies of the enol tautomers with respect to the keto forms. The first number is for calculation at the B3LYP/6-311++G** level, and the second number is for calculation at the MP2/cc-pVTZ level.

analysis, we conclude that the contribution of methyl hyperconjugation energy with an adjacent ethylenic group in the enolic form of a 2-methyl ketone is ~2 kcal/mol.

(iii) Becasue the site of the methyl group in the A3 tautomer (the system of concern in the present study) is similar to that in species IV$_{enol}$, the contributions of methyl hyperconjugation energy to the stabilities of the two enolic species can be considered to be similar, i.e., ~2 kcal/mol. Therefore, the excess stability of A3 over A2 (~1.5 kcal/mol) must originate from the contributions of CH···O H-bonding and a cooperative interaction between the two said hydrogen bonds.

4. Summary

The results of the combined study of matrix-isolation FTIR spectroscopy and electronic structure calculations on CD and 3-MeCD presented here demonstrate stabilization of a monoenol tautomer of the latter molecule through the cooperative interaction of an intramolecular O—H···O HB with an interconnected C—H···O counterpart, where a methyl C—H bond is the HB donor. In the FTIR spectra, the enhanced stabilization of that enol tautomer is manifested as a red-shifted ν_{OH} transition frequency and larger spectral bandwidth compared to that of CD. The ν_{CH} band corresponding to the methyl C—H group involved in the C—H···O H-bonding with enolic oxygen has been identified. A comparison of the theoretical infrared spectrum of this tautomeric species with that of an analogous molecule (4-MeCED) reveals that the ν_{C-H} band of the C—H···O H-bonded methyl C—H bond is significantly blue-shifted. NBO analysis also indicates the existence of the intramolecular C—H···O HB and its cooperative interaction with the interconnected O—H···O HB. To our knowledge, this result is the first spectroscopic evidence of a correlation between two intramolecular HBs where one of them is of the weak C—H···O type.

Acknowledgment. The authors acknowledge financial support received from the Ramanna Fellowship Grant of the Department of Science and Technology, Government of India, to carry out the research, and also the partial support received from the council of Scientific and Industrial Research (CSIR), Government of India. P.P. and B.B. thank the CSIR for SRF grants.

Supporting Information Available: Fully optimized geometries of all structures, total energies, ZPEs, Mulliken charges, natural charges on donor—acceptor atoms, hybridizations of carbon atoms of three methyl C—H bonds, values of hyperconjugation energy and details of its evaluation, variations in the energy of the A3 tautomer as a function of internal rotation of the methyl group, and hyperconjugation interaction energy as a function of internal rotation of the methyl group. This material is available free of charge via the Internet at http://pubs.acs.org.

References and Notes

(1) Desiraju, G. R.; Steiner, T. *The Weak Hydrogen Bond*; Oxford University Press: New York, 1999.
(2) Scheiner, S. *Hydrogen Bonding: A Theoretical Perspective*; Oxford University Press: New York, 1997.
(3) Karpfen, A. *Adv. Chem. Phys.* **2002**, *123*, 469–510.
(4) Parra, R. D.; Ohlssen, J. *J. Phys. Chem. A* **2008**, *112*, 3492–3498.
(5) Buck, U.; Huisken, F. *Chem. Rev.* **2000**, *100*, 3863–3890.
(6) Ohno, K.; Okimura, M.; Akai, N.; Katsumoto, Y. *Phys. Chem. Chem. Phys.* **2005**, *7*, 3005–3014.
(7) Wieczorek, R.; Dannenberg, J. J. *J. Am. Chem. Soc.* **2003**, *125*, 8124–8129.
(8) Chen, Y.; Dannenberg, J. J. *J. Am. Chem. Soc.* **2006**, *128*, 8100–8101.
(9) Karpfen, A.; Kryachko, E. S. *J. Phys. Chem. A* **2007**, *111*, 8177–8187.
(10) Raveendran, P.; Wallen, S. L. *J. Am. Chem. Soc.* **2002**, *124*, 12590–12599.
(11) Steiner, T.; Lutz, B.; van der Mass, J.; Veldman, N.; Schreurs, A. M. M.; Kroon, J.; Kanters, J. A. *Chem. Commun.* **1997**, 191–192.
(12) Steiner, T. *Cryst. Rev.* **1996**, *6*, 1–57.
(13) Gatti, C.; May, E.; Destro, R.; Cargnoni, F. *J. Phys. Chem. A* **2002**, *106*, 2707–2720.
(14) Blatchford, M. A.; Raveendran, P.; Wallen, S. L. *J. Am. Chem. Soc.* **2002**, *124*, 14818–14819.
(15) Giambiagi, M. S.; Neto, M. O.; Neder, A. V. F. *J. Math. Chem.* **2005**, *38*, 519–532.
(16) Kazuhiko, H.; Kuwae, A.; Kawai, S.; Ono, Y. *J. Phys. Chem.* **1989**, *93*, 6013–6016.
(17) Nowak, M. J.; Lapinski, L.; Fulara, J.; Les, A.; Adamowicz, L. *J. Phys. Chem.* **1992**, *96*, 1562–1569.
(18) Schiavoni, M. M.; Mack, H.-G.; Ulic, S. E.; Della Vedova, C. O. *Spectrochim. Acta Part A* **2000**, *56*, 1533–1541.
(19) Raczynska, E. D.; Duczmal, K.; Darowska, M. *Vib. Spectrosc.* **2005**, *39*, 37–45.
(20) Sloop, J. C.; Bumgardner, C. L.; Washington, G.; Loehle, W. D.; Sankar, S. S.; Lewis, A. B. *J. Fluorine Chem.* **2006**, *127*, 780–786.

(21) Gianturco, M. A.; Giammarino, A. S.; Pitcher, R. G. *Tetrahedron* **1963**, *19*, 2051–2059.
(22) Francis, J. T.; Hitchcock, A. P. *J. Phys. Chem.* **1994**, *98*, 3650–3657.
(23) Bouchoux, G.; Hoppilliard, Y.; Houriet, R. *New J. Chem.* **1987**, *11*, 225–233.
(24) Shen, Q.; Traetteberg, M.; Samdal, S. *J. Mol. Struct.* **2009**, *923*, 94–97.
(25) Frisch, M. J.; Trucks, G. W.; Schlegel, H. B.; Scuseria, G. E.; Robb, M. A.; Cheeseman, J. R.; Montgomery, J. A., Jr.; Vreven, T.; Kudin, K. N.; Burant, J. C.; Millam, J. M.; Iyengar, S. S.; Tomasi, J.; Barone, V.; Mennucci, B.; Cossi, M.; Scalmani, G.; Rega, N.; Petersson, G. A.; Nakatsuji, H.; Hada, M.; Ehara, M.; Toyota, K.; Fukuda, R.; Hasegawa, J.; Ishida, M.; Nakajima, T.; Honda, Y.; Kitao, O.; Nakai, H.; Klene, M.; Li, X.; Knox, J. E.; Hratchian, H. P.; Cross, J. B.; Bakken, V.; Adamo, C.; Jaramillo, J.; Gomperts, R.; Stratmann, R. E.; Yazyev, O.; Austin, A. J.; Cammi, R.; Pomelli, C.; Ochterski, J. W.; Ayala, P. Y.; Morokuma, K.; Voth, G. A.; Salvador, P.; Dannenberg, J. J.; Zakrzewski, V. G.; Dapprich, S.; Daniels, A. D.; Strain, M. C.; Farkas, O.; Malick, D. K.; Rabuck, A. D.; Raghavachari, K.; Foresman, J. B.; Ortiz, J. V.; Cui, Q.; Baboul, A. G.; Clifford, S.; Cioslowski, J.; Stefanov, B. B.; Liu, G.; Liashenko, A.; Piskorz, P.; Komaromi, I.; Martin, R. L.; Fox, D. J.; Keith, T.; Al-Laham, M. A.; Peng, C. Y.; Nanayakkara, A.; Challacombe, M.; Gill, P. M. W.; Johnson, B.; Chen, W.; Wong, M. W.; Gonzalez, C.; Pople, J. A. *Gaussian 03*, revision E01; Gaussian, Inc.: Wallingford, CT, 2004.
(26) Bernath, P. F. *Spectra of Atoms and Molecules*; Oxford University Press: New York, 1995.
(27) Cremer, D.; Binkley, J. S.; Pople, J. A.; Hehre, W. J. *J. Am. Chem. Soc.* **1974**, *96*, 6900–6903.
(28) Hobza, P.; Havlas, Z. *Chem. Rev.* **2000**, *100*, 4253–4264.
(29) van der Veken, B. J.; Herrebout, W. A.; Szostak, R.; Shchepkin, D. N.; Havlas, Z.; Hobza, P. *J. Am. Chem. Soc.* **2001**, *123*, 12290–12293.
(30) Hobza, P.; Havlas, Z. *Theor. Chem. Acc.* **2002**, *108*, 325–334.
(31) Delanoye, S. N.; Herrebout, W. A.; van der Veken, B. J. *J. Am. Chem. Soc.* **2002**, *124*, 7490–7498.
(32) Delanoye, S. N.; Herrebout, W. A.; van der Veken, B. J. *J. Am. Chem. Soc.* **2002**, *124*, 11854–11855.
(33) Qian, W.; Krimm, S. *J. Phys. Chem. A* **2002**, *106*, 6628–6636.
(34) Li, X.; Liu, L.; Schlegel, H. B. *J. Am. Chem. Soc.* **2002**, *124*, 9639–9647.
(35) Barnes, A. J. *J. Mol. Struct.* **1997**, 436–437, 167−171.
(36) Barnes, A. J. *J. Mol. Struct.* **2004**, *704*, 3–9.
(37) Buckingham, A. D.; Del Bene, J. E.; McDowell, S. A. C. *Chem. Phys. Lett.* **2008**, *463*, 1–10.
(38) Joseph, J.; Jemmis, E. D. *J. Am. Chem. Soc.* **2007**, *129*, 4620–4632.
(39) Dykstra, C. E. *Acc. Chem. Res.* **1988**, *21*, 355–361, and references therein.
(40) Scheiner, S.; Grabowski, S. J.; Kar, T. *J. Phys. Chem. A* **2001**, *105*, 10607–10612.
(41) Mukhopadhyay, A.; Mukherjee, M.; Pandey, P.; Samanta, A. K.; Bandyopadhyay, B.; Chakraborty, T. *J. Phys. Chem. A* **2009**, *113*, 3078–3087.
(42) Reed, A. E.; Curtiss, L. A.; Weinhold, F. *Chem. Rev.* **1988**, *88*, 899–926.
(43) Alabugin, I. V.; Manoharan, M.; Peabody, S.; Weinhold, F. *J. Am. Chem. Soc.* **2003**, *125*, 5973–5987.
(44) Florio, G. M.; Zwier, T. S.; Myshakin, E. M.; Jordan, K. D.; Sibert, E. L., III. *J. Chem. Phys.* **2003**, *118*, 1735–1746.
(45) Hazra, M. K.; Chakraborty, T. *J. Phys. Chem. A* **2008**, *112*, 1100–1104.

JP907881B